PNAS RESEARCH ARTICLE | MICROBIOLOGY OPEN ACCESS

ACOD1-mediated lysosomal membrane permeabilization contributes to *Mycobacterium tuberculosis*–induced macrophage death

Ziwei Yang[a,1], Li Zhang[b,1], Samantha Ottavi[c], Jacob B. Geri[d], Andrew Perkowski[c], Xiuju Jiang[a], Daniel Pfau[a], Ruslana Bryk[a], Jeffrey Aubé[c], Matthew Zimmerman[e], Véronique Dartois[e], and Carl Nathan[a,2]

Affiliations are included on p. 10.

Contributed by Carl Nathan; received December 3, 2024; accepted February 18, 2025; reviewed by Katherine A. Fitzgerald, Anne O'Garra, and Sarah A. Stanley

Mycobacterium tuberculosis **(Mtb) primarily infects macrophages. In vitro without antibiotics, wild-type Mtb hastens death of the macrophages, but the processes leading to rapid cell death are not well understood. Our earlier work indicated that the death of Mtb-infected mouse macrophages in vitro is markedly exacerbated by induction of interferon-β (IFN-β) [L. Zhang et al., *J. Exp. Med.* 18, e20200887 (2021)]. Here, we identified a key downstream response to IFN-β in the context of Mtb infection as the massive induction of cis-aconitate decarboxylase (ACOD1), not only in its canonical subcellular localization in mitochondria but also in the cytosol, where it bound to the lysosome-stabilizing protein HSP70. ACOD1's product, itaconate, protected Mtb-infected macrophages. However, the contrasting and predominant effect of high-level ACOD1 expression was to act in a noncatalytic manner to promote HSP70's degradation, leading to lysosomal membrane permeabilization (LMP). Mtb-induced macrophage death was markedly diminished by inhibitors of cysteine proteases, consistent with lysosome-mediated cell death. Neither ACOD1 inhibitors nor cysteine protease inhibitors are suitable for potential host-directed therapy (HDT) of tuberculosis. Instead, this work directs attention to how ACOD1 acts nonenzymatically to promote the degradation of HSP70.**

ACOD1 | IRG1 | lysosomes | tuberculosis | macrophages

Significance

Here, we show that when Mtb induces macrophages to express interferon-β (IFN-β), they overexpress an enzyme called ACOD1 normally found in mitochondria, whose product, itaconate, protects the cells. Surprisingly, that protective effect is overwhelmed by a nonenzymatic action of ACOD1 acting in the cytosol, where ACOD1 promotes the degradation of HSP70, a protein that protects lysosomes. Without HSP70's protective effect, cysteine proteases leak from (phago)lysosomes in Mtb-infected macrophages and contribute to death of the cells. These findings focus attention on uncharacterized protein–protein interactions of ACOD1 as potential points of intervention.

Tuberculosis remains a leading cause of death from infection. Early after *Mycobacterium tuberculosis* (Mtb) enters a new host, most of the Mtb are contained in macrophages and prevented from causing clinically apparent disease. In a minority of people infected with Mtb, the bacterium eventually succeeds in killing macrophages, spreading to other macrophages and proliferating. Tissue breakdown can then ensue, along with aerosol transmission to other hosts, with or without the onset of clinical illness.

In view of the gate-keeper role of macrophages, there is intense interest in the mode of Mtb-induced macrophage cell death. Studies in vitro have highlighted a variety of mechanisms (1). Their variable predominance in different studies is not understood, although variation in multiplicity of infection (MOI) may influence the outcome. In our hands, a CRISPR-Cas9 knockout screen led to the conclusion that the death of Mtb-infected mouse macrophages under the conditions studied was substantially dependent on type I IFN that the macrophages produced in response to Mtb (1). IFN-β also hastened the death of human monocyte–derived macrophages (2). However, IFN-β itself did not kill uninfected macrophages. We therefore refer to this phenomenon as macrophage death co-dependent on Mtb and type I IFN signaling (Co-D MD). Co-D MD did not appear to proceed by apoptosis, pyroptosis, necroptosis, or ferroptosis (1). The possible pathophysiologic relevance of type I IFN-augmented macrophage death was supported by the ability of anti-IFNAR to protect mice from Mtb (1). However, anti-IFNAR would not be an acceptable adjunctive host-directed therapy (HDT) for TB, because it would predispose to viral infection (3–5).

Here, we used orthogonal genetic and biochemical approaches to identify key players downstream of IFNAR signaling that might mediate Co-D MD without being required for antiviral activity. In the genetic approach, we identified genes whose expression was induced at an early time point in infected vs uninfected wild-type (WT) and *Ifnar1*$^{-/-}$ mouse bone marrow–derived macrophages (BMDM). We then carried out two CRISPRa screens in *Ifnar2*$^{-/-}$ RAW 264.7 macrophages—one screen with a genome-wide sgRNA library and the other with a library of the genes we refer to as type I IFN-stimulated (ISGs) because their induction during Mtb infection was dependent on IFNAR. We identified the genes whose transcriptional activation

Author contributions: Z.Y., L.Z., J.A., and C.N. designed research; Z.Y., L.Z., S.O., J.B.G., X.J., D.P., M.Z., and V.D. performed research; J.B.G., A.P., and J.A. contributed new reagents/analytic tools; Z.Y., L.Z., S.O., J.B.G., and R.B. analyzed data; and Z.Y. and C.N. wrote the paper.

Reviewers: K.A.F., University of Massachusetts Medical School; A.O., The Francis Crick Institute; and S.A.S., University of California Berkeley.

The authors declare no competing interest.

[1]Z.Y. and L.Z. contributed equally to this work.

[2]To whom correspondence may be addressed. Email: cnathan@med.cornell.edu.

This article contains supporting information online at https://www.pnas.org/lookup/suppl/doi:10.1073/pnas.2425309122/-/DCSupplemental.

Published March 18, 2025.

increased the death of Mtb-infected *Ifnar2*$^{-/-}$ macrophages in both screens. Among these, we focused on one gene that encodes a protein that we found to be markedly increased in cells that were soon to undergo Co-D MD. This was cis-aconitate decarboxylase-1 (ACOD1), also called immune-responsive gene 1 (IRG1).

In the biochemical approach, we tested a variety of inhibitors and found that calpain inhibitor XII (CI-XII) diminished and delayed Co-D MD. We used an advanced affinity labeling technique (6) based on CI-XII to identify its targets. Surprisingly, no calpains were among the proteins pulled down, nor was knockout of calpain-1 protective. Instead, derivatized CI-XII bound to a variety of lysosomal proteases. Knockout of individual proteases did not protect the cells from Co-D MD, but macrophages were protected from Co-D MD by a pan-cathepsin inhibitor, K777. This led us to recognize that our earlier evidence excluding multiple known forms of cell death (1) had not considered a pathway called lysosome-dependent cell death (7), which can follow lysosome membrane permeabilization (LMP). LMP is commonly seen in stressed cells (8). When LMP is sublethal, lysosomal repair and biogenesis can follow activation of the TFEB-mTORC1 pathway (9), while more severe LMP can lead to release into the cytosol of cathepsins and other lysosomal enzymes, followed by death of the cell (10).

We then faced the puzzle how ACOD1, a mitochondrial enzyme that produces itaconate (11), might lead to LMP. We found that when ACOD1 is highly expressed in macrophages, it accumulates in the cytosol, where it associates with HSP70. Moreover, we found that ACOD1 played two opposing roles in Co-D MD. Production of itaconate protected the macrophages. In contrast, acting in a dominant, noncatalytic mode, ACOD1 promoted lysosome-dependent cell death. This may be related to its association with and promotion of the proteasomal degradation of HSP70, a lysosome-stabilizing protein (12–15).

Results

ACOD1 Is Highly Expressed in Mtb-Infected Macrophages. We infected WT and *Ifnar1*$^{-/-}$ BMDM on the C57BL/6 background with Mtb H37Rv at a MOI of 10 and kept other cells uninfected. We also studied infected and uninfected BMDM from mice on the 129S2 and 129X1 backgrounds. At 24 h postinfection (p.i.), which is at least 2 d before Co-D MD becomes apparent under these conditions, we lysed the cells for RNAseq analysis (Fig. 1*A*). The upregulation of 798 genes was type I IFN-dependent [with $\log_2$ (fold-change) $_{\text{WT-Mtb vs WT}}$ − $\log_2$ (fold-change)$_{\text{KO-Mtb vs KO}}$ of >1] (Fig. 1*B* and *SI Appendix*, Fig. S1 *A* and *B*). To determine whether any of these genes mediate Co-D MD, we used CRISPRa to overexpress them in *Ifnar2*$^{-/-}$ RAW264.7 macrophages, infected the pooled cells with Mtb, and used deep sequencing to identify which of the corresponding sgRNAs were most extensively deleted from the pool. Given that other ISGs might play a role whose expression peaked earlier or later than the time point chosen for RNAseq, we independently conducted another CRISPRa screen using a genome-wide sgRNA library. The results are illustrated in Fig. 1*C* and the genes are listed in Dataset S2. We then asked which genes were candidates for mediating Co-D MD in both screens. Among those, ACOD1 (Fig. 1*C*) drew our attention because of the prominent role of its product, the electrophilic metabolite itaconate, in modulating macrophage signaling pathways (14), coinducing IFN-β (15) and activating TFEB (16), a transcription factor that helps macrophages control Mtb (17).

Mtb infection markedly increased expression of ACOD1 at the protein level both in BMDM (Fig. 1*D*) and in RAW264.7 cells (*SI Appendix*, Fig. S1*C*). Both BMDM and RAW264.7 cells also expressed high levels of ACOD1 when stimulated with lipoteichoic acid from *S. aureus* (LTA-SA), which, like Mtb, is a TLR2 agonist (*SI Appendix*, Fig. S1*D*). These results are reminiscent of the observations of Bomfim et al. that Mtb induces ACOD1 in macrophages via combined signals from TLR2 and IFNAR, the latter triggered

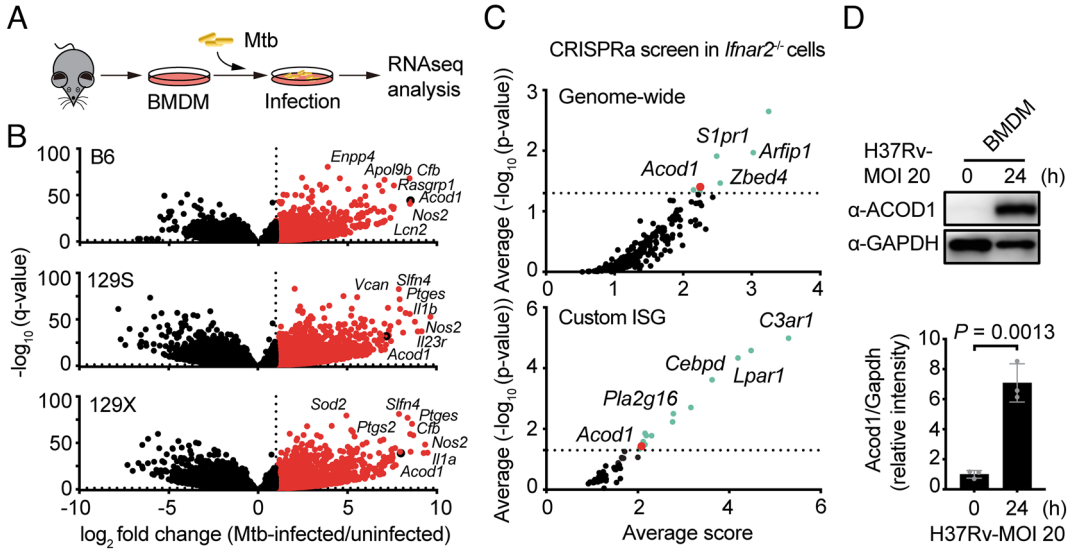

Fig. 1. ACOD1 is upregulated upon Mtb infection and is a candidate for contributing to Mtb-induced macrophage death. (*A*) Schematic representation of the RNA sequencing workflow for BMDM. (*B*) Volcano plots of the transcription level of genes from Mtb H37Rv-infected versus uninfected BMDM 24 h postinfection (h.p.i). The dashed line indicates $\log_2$ fold change = 1. B6, 129S2 and 129X1: mouse strains. (*C*) Candidate gene hits from a genome-wide or custom ISG CRISPRa screen of Mtb-induced RAW264.7 *Ifnar2*$^{-/-}$ cell death. Shown are genes whose upregulation promotes cell death (negative screen) from three replicate experiments, where the x axis shows the calculated score using negative binomial distribution, and the y axis represents the statistical analysis. (*D*) (*Top*) Immunoblot analysis of BMDM infected with Mtb H37Rv for 24 h at a multiplicity of infection (MOI) of 20. (*Bottom*) semiquantification of indicated protein levels, assessed by gray intensity analysis via Image J software. Data in D show mean ± SD of triplicates in 1 experiment representative of 3 independent experiments. *P*-value by the unpaired *t* test.

by STING, when STING is activated by Mtb products escaping the phagosome to the cytosol in an ESX-1-dependent manner (18). We then compared the level of ACOD1 at the protein level in RAW264.7 cells transfected with *Acod1* under a TRE promoter to the level of ACOD1 in cells transfected with an empty vector (EV) and then infected with Mtb. The induction of ACOD1 by Mtb infection was even greater than seen with vector-driven overexpression (*SI Appendix*, Fig. S1*E*).

ACOD1 Regulates Mtb-Induced Cell Death. To assess ACOD1's impact on the viability of Mtb-infected cells, we overexpressed *Acod1* or EV in BMDM by lentiviral transduction. High-level expression of ACOD1 did not itself decrease cell viability (*SI Appendix*, Fig. S2), but augmented the cell death caused by infection with Mtb (Fig. 2*A*). Next, we turned to BMDM from *Acod1*$^{-/-}$ mice. However, the precursor bone marrow cells from *Acod1*$^{-/-}$ mice proliferated much more slowly than WT cells in CSF1-containing medium. The resulting BMDM were smaller than those from WT mice and their survival in culture without Mtb infection was as poor as that of macrophages from WT mice after Mtb infection (Fig. 2*B*). The sickly baseline state of A*cod1*$^{-/-}$ BMDM made it difficult to interpret the further decrease in viability seen when the cells were infected with Mtb (Fig. 2 *B* and *C*).

Given that we could not use *Acod1*$^{-/-}$ BMDM, we turned to RAW264.7 macrophages overexpressing or lacking ACOD1. When *Acod1* was overexpressed in RAW264.7 cells, Mtb decreased cell viability more than in RAW264.7 cells transfected with EV (Fig. 2*D*). Conversely, knocking out *Acod1* alleviated Mtb-induced cell death (Fig. 2*E*). Hereafter, "WT" refers to BMDM derived from wild-type mice, while "NC" (negative control) denotes a clone of RAW264.7 cells carried through most of the steps used for gene modification but without any gene modification.

Certain Protease Inhibitors Protect Cells from Mtb-Induced Cell Death. While the CRISPRa screens were underway, we continued to screen inhibitors for their ability to decrease Co-D MD. Among them was a peptidyl α-keto amide called calpain-1 inhibitor CI-XII (19) which was included because calpain, a calcium-dependent, cytosolic cysteine protease, can play a role in cell death (20) and in the proteolytic inactivation of inducible nitric oxide synthase (iNOS) (21). CI-XII afforded complete protection against Co-D MD (Fig. 3*A*). The broad-spectrum protease inhibitor E64D (22) protected as well, but less extensively and less durably than CI-XII.

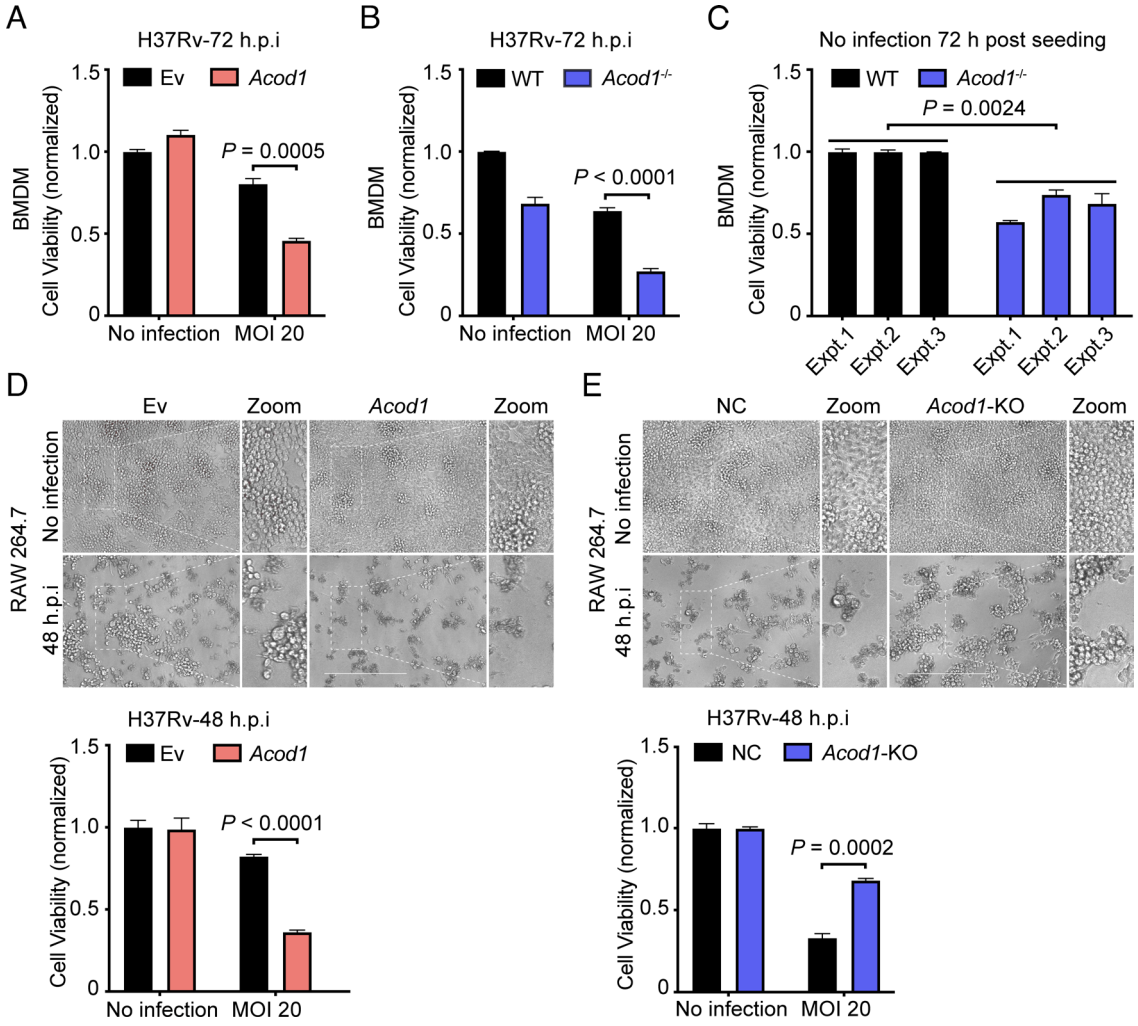

Fig. 2. ACOD1 influences Mtb-induced cell death. (*A*) WT BMDM were infected with Ev- or *Acod1*-encoding lentivirus, then infected or not with Mtb H37Rv at MOI 20 for the indicated times. Cell viability was assessed by ATP assay. (*B*) WT and *Acod1*$^{-/-}$ BMDM were infected with Mtb H37Rv and viability assessed as in (*A*). (*C*) Cell viability comparison of different batches of uninfected WT and *Acod1*$^{-/-}$ BMDM, assessed by ATP assay. (*D*) Ev- or ACOD1-overexpressing RAW264.7 cells were infected with Mtb H37Rv and cell viability assessed by microscopy (*Top*; Scale bar, 300 μm) and ATP assay (*Bottom*). (*E*) Negative control (NC, nonspecific guide RNA transfected cells) and *Acod1*-knock out (*Acod1*-KO) RAW264.7 cells were infected with Mtb H37Rv and cell viability assessed by microscopy (*Left*; scale bar, 300 μm) and ATP assay (*Right*). Data in *A*–*E* represent mean ± SD of 3 replicates in 1 experiment representative of 2 (*A*) or 3 (*B*–*E*) independent experiments. *P*-values by the unpaired *t* test.

No protection was seen with additional inhibitors of calpain 1 and/or calpain 2 called CI-II and CI-III (21) or inhibitors of cathepsin B (CA074-ME) (23), cathepsins B and L (CI-II) (24), cathepsins D and E (pepstatin A) (25), cathepsin G[(2-(3-((1-benzoylpiperidin-4-yl)(methyl)carbamoyl)naphthalen-2-yl)-1-(naphthalen-1-yl)-2-oxoethyl)phosphonic acid] (26), or cathepsin S (Clik60) (27). The reported inhibitory profiles for these compounds are listed in *SI Appendix*, Table S1, but may not reflect the full range of their activities in cells. BMDM from calpain $1^{-/-}$ mice underwent Co-D MD that was no different in extent than those from WT mice. Moreover, calpain $1^{-/-}$ BMDM were equally well protected by CI-XII as WT cells (Fig. 3*B*), and results were similar in RAW264.7 cells in which we knocked out cathepsins S or B (*SI Appendix*, Fig. S3*A*). We concluded that more than one cysteine protease likely acts redundantly, and CI-XII could be a useful tool to identify them.

CI-XII Binds Cathepsins S, B, and Z and Prolyl-X-Carboxypeptidase in Mtb-Infected BMDM. To determine what proteins are targeted by CI-XII, we synthesized a variety of analogs with a diazirene moiety whose photoactivation would lead to cross-linking to associated proteins. However, these analogs had markedly reduced efficacy in protecting BMDM from Co-D MD and the proteins they pulled down were both extremely numerous and variable across experiments (data not shown). We then synthesized an analog of CI-XII with a covalently attached moiety that chelates iridium (*SI Appendix*, Fig. S3*B*). We incubated the probe with intact Mtb-infected BMDM or their preformed lysates and with macrophage-free lysates of Mtb, with diazirene-biotin present in each case. After irradiation with 450 nm light, the iridium engages in Dexter energy transfer to the diazirene-biotin, causing a carbene to form on the diazirine, whose short half-life limits covalent crosslinking to proteins within 4 nanometers (40 Å) of the iridium probe (5), identifiable using streptavidin immunoprecipitation followed by mass spectrometry (Fig. 3*C*). We used competition with unmodified CI-XII to distinguish specific from nonspecific interactions of the CI-XII probe (Fig. 3*C*). Peptide fingerprinting by timsTOF mass spectrometry then identified proteins closely associated with the CI-XII probe. Two Mtb proteins were identified from Mtb lysate. However, when BMDM were infected with their transposon mutants, CI-XII remained functional in inhibiting Mtb-induced cell death (*SI Appendix*, Fig. S3*C*), implying that the functionally relevant target(s) of CI-XII is/are in the macrophage, not in Mtb. Remarkably, this analysis did not identify calpain-1 from BMDM, whether the cells were lysed by sonication or with detergent. Calpain-5 was identified as a potential target in a detergent lysate of BMDM, but not at a statistically significant level. Instead, cathepsins S (CATS), B (CATB), and Z (CATZ) and lysosomal pro-X carboxypepdidase (PCP) were the enzymes identified as CI-XII targets with highest confidence (Fig. 3*D*). Neither the CATZ inhibitor X-IN-I (29) nor the PCP inhibitor (compound 4) (30) protected Mtb-infected BMDM from Co-D MD (*SI Appendix*, Fig. S3 *D* and *E*), and knockout of *Ctsz* and *Prcp* from RAW264.7 cells left them as vulnerable to Co-D MD as control cells (*SI Appendix*, Fig. S3 *F* and *G*). Analysis of the alignment of CATS, CATB, and CATZ with the protein sequence of calpain 1 (Fig. 3*E*, *Left*) and docking of calpain 1 inhibitor SNJ-1945 (31) in the calpain 1 crystal structure offered supporting evidence that CI-XII likely binds the active sites not only of calpain 1 but also of CATS, CATB, and CATZ, where covalent bonds are likely to form with amino acids 147C of CATS (Fig. 3*E*, *Right*), 108C of CATB, 94C of CATZ, and 115C of calpain 1 (CAN1) (*SI Appendix*, Fig. S3*H*). In addition, a polar contact with CI-XII is postulated with amino acids 192G of CATS (Fig. 3*E*, *Right*), 153G of CATB, 137G of CATZ, and 208G of CAN1 (*SI Appendix*, Fig. S3*H*). These findings strongly supported the hypothesis that multiple cysteine proteases mediate Co-D MD. At the same time, the failure of the CI-XII-based probe to pull down calpain 1 was strong evidence that the list of candidates obtained through the pull-down approach was incomplete. Given that there are ~150 cysteine proteases, including 12 cysteine cathepsins, this dissuaded us from attempting to create compound knockouts and encouraged us instead to test an additional inhibitor with a broader known range of cysteine protease targets.

Pan-Cathepsin Inhibitor K777 Protects Cells from Mtb-Induced Cell Death. The peptidyl vinyl sulfone K777 is known to inhibit CATS, CATZ, CATB, and CATL (32–35). K777 protected BMDM against Mtb-induced cell death to the same extent as CI-XII (Fig. 3 *F* and *G*) and was more potent in doing so (Fig. 3*H*). K777 also protected RAW264.7 cells (Fig. 3*I*), but to a lesser extent, perhaps because 10 μM concentrations of CI-XII and K777 only partially suppressed the activities of CATS and CATB in RAW264.7 cells (Fig. 3 *J* and *K*).

High Levels of ACOD1 Mediate LMP. Next, we sought to understand what might link the high-level expression of ACOD1 in Mtb-infected macrophages to a cell death pathway apparently dependent on cysteine proteases that are chiefly but not exclusively expressed in lysosomes. We first sought to monitor the effect of Mtb infection on levels of the lysosomal membrane stability-conferring protein HSP70 (12, 13, 36–38) and the lysosomal biogenesis-promoting transcription factor TFEB (9). As Mtb infection increased levels of ACOD1 in RAW264.7 cells, it decreased levels of HSP70 and TFEB (Fig. 4*A*). To test whether these changes might be associated with LMP, we checked for redistribution of galectin-3 from cytosol to lysosomes, where galectin-3 can bind proteins associated with the internal face of the lysosomal membrane (39–41). Indeed, punctate formation of tagged galectin 3 upon *Acod1* overexpression in RAW264.7 cells and colocalization of galectin 3 with the lysosomal membrane protein LAMP1 (Fig. 4 *B* and *C*) implied that high levels of ACOD1 lead to LMP. Consistent with that, ACOD1 overexpression caused loss of lysosomal concentration of the pH-sensitive dye pHLysRed, as inferred from the mean fluorescence intensity of each cell analyzed (Fig. 4 *D* and *E*). This suggested possible redistribution of CATS, CATB, and CATZ from lysosomes to cytosol (Fig. 4*D*). While we did not consistently see an increase in cathepsins in the cytosol, where they preexist, we did see redistribution of LAMP1 from the lysosome-enriched fraction to the cytosolic fraction when *Acod1* was overexpressed (Fig. 4*F*), but not when *Acod1* was deleted (Fig. 4*G*). There did not appear to be a reduction in overall lysosome number, because *Acod1* overexpression or knockout had no impact on levels of LAMP1 mRNA and did not decrease total LAMP1 protein levels in unfractionated cell lysates (Fig. 4*H*). Moreover, when *Acod1* was overexpressed, HSP70, CATS, CATB, and CATZ decreased in the lysosomal compartment (Fig. 4*I*), along with LAMP1 (Fig. 4*F*). Conversely, the lysosomal fraction contained more HSP70, CATS, and CATB and an unaltered level of CATZ in *Acod1*$^{-/-}$ cells compared to wild-type cells (Fig. 4*J*). We conclude that the levels of ACOD1 seen in Mtb-infected macrophages can lead to LMP.

Cytosolic ACOD1 Associates with HSP70 and Decreases Its Levels. An immunofluorescent assay showed that when ACOD1 was expressed to a high level in Mtb-infected BMDM, much of it was present in the cytosol (Fig. 5*A*). The same was true in RAW264.7 cells in which ACOD1 was overexpressed (Fig. 5*B*).

HSP70 is also cytosolic. Direct evidence for their interaction came from coimmunoprecipitation of ACOD1 and HSP70 with anti-HSP70 antibody (Fig. 5 *B* and *C*), and reciprocal experiments with anti-ACOD1 antibody (*SI Appendix*, Fig. S4*A*) in RAW264.7 cells or with anti-HA antibody in HEK293T cells transfected with HA-tagged ACOD1 (*SI Appendix*, Fig. S4*B*) as well. Addition of cycloheximide (CHX) to block nascent protein synthesis revealed that ACOD1 overexpression led to a rapid and profound decrease in the level of preformed HSP70 (Fig. 5*D*). Conversely, when ACOD1 was absent, HSP70's levels were maintained in the absence of new synthesis (Fig. 5*E*). The proteasome inhibitor MG-132 prevented the ACOD1-mediated decrease in HSP70 levels, while treating cells with the autophagy inhibitors 3-methyladenine (3-MA), chloroquine (4), or NH_4Cl did not (*SI Appendix*, Fig. S4*C*). Carfilzomib, an inhibitor that is more highly selective for the proteasome than MG-132 (42, 43), also prevented the ACOD1-mediated decrease in HSP70 (*SI Appendix*, Fig. S4*D*). In *Acod1*$^{-/-}$ cells, MG-132 had no effect on HSP70 levels (*SI Appendix*, Fig. S4*E*). Thus, ACOD1 associates with HSP70 and promotes its marked decrease in abundance, apparently by proteasomal degradation.

ACOD1 Acts Noncatalytically to Promote Degradation of HSP70. ACOD1 could potentially affect macrophage viability in four ways—through consumption of cis-aconitate; production of itaconate; production of CO_2, possibly leading to acidification of the mitochondrial compartment in which ACOD1 resides and disrupting the proton-motive force (44); or by a noncatalytic mechanism. K207A and H103A muteins of ACOD1 are unable to catalyze decarboxylation of cis-aconitate (45). Accordingly, we constructed K207A and H103A mutants and overexpressed EV, WT-ACOD1, K207A-ACOD1, or H103A-ACOD1 in RAW264.7 cells. The enzyme-dead ACOD1 muteins were as effective as WT ACOD1 in promoting degradation of HSP70 (Fig. 5*F*). Moreover, treatment of the cells with membrane-permeable 4-octyl-itaconate (4OI) had no detectable impact on HSP70 levels, whether or not ACOD1 was present (*SI Appendix*, Fig. S4 *F*, *G*, and *H*).

ACOD1 Promotes LMP and Mtb-Induced Cell Death Independently of Itaconate. Having learned that ACOD1 acts noncatalytically to promote degradation of HSP70, we next asked whether ACOD1 also acts noncatalytically to promote LMP and Mtb-induced cell death. We overexpressed K207A-ACOD1, H103A-ACOD1, WT-ACOD1, or GFP as a control in *Ifnar2*$^{-/-}$ cells. After infection with Mtb for 48 h, when compared to the extent of death induced by Mtb in GFP-overexpressing cells, Mtb induced even greater death in cells expressing either WT ACOD1 or the enzyme-dead ACOD1 muteins, and to a similar extent in each case (Fig. 6*A*).

This result appears to stand at odds with the ability of itaconate to promote nuclear localization of TFEB, lysosomal biogenesis, and improved cell viability during bacterial infection (46). Indeed, when we added cell membrane-permeable 4-OI to Mtb-infected cells, their viability was promoted beyond the level of protection provided by knockout of *Acod1* (Fig. 6*B*). Moreover, 4-OI protected *Acod1*$^{-/-}$ BMDM from Mtb-induced cell death as well as boosted the viability of these sickly cells in the absence of Mtb infection (Fig. 6*C*). Cytotoxicity of 4-OI (Fig. 6*D*) and protection of WT BMDM from Mtb-induced cell death by 4-OI (Fig. 6*E*) were both concentration-dependent. Protection was first detectable, albeit at a minimal level, with 8 μM 4-OI and greatest at the highest concentration of 4-OI (250 μM) that was not cytotoxic. Although the levels of 4-OI that afforded substantial protection may not be physiologic (11), we conclude that ACOD1 may play a bifunctional role in Mtb-infected macrophages, with a catalytic action opposing, but not overcoming, a noncatalytic action.

Role of Increased Mitochondrial ACOD1 in Mtb-Infected Cells. ACOD1 is considered to reside mainly in mitochondria (47, 48), but we found that its overexpression in macrophages led to abundant expression in the cytosol (Fig. 5*A*). Given ACOD1's ability to play distinct and opposing roles after Mtb infection, we next compared the impact of Mtb infection and ACOD1 overexpression on ACOD1's subcellular distribution in mitochondria and cytosol, keeping in mind that forced overexpression leads to levels that are lower than or just equivalent to Mtb infection (Fig. 1*D* and *SI Appendix*, Fig. S1 *C* and *E*). Immunofluorescent analysis supported mitochondrial localization (*SI Appendix*, Fig. S5*A*) as well as cytosolic localization but did not suggest colocalization with the lysosome marker LAMP1 (*SI Appendix*, Fig. S5*B*). Cell fractionation followed by immunoblotting showed that Mtb infection and overexpression each increased ACOD1 levels in both mitochondria and cytosol (*SI Appendix*, Fig. S5*C*), as did treatment with the TLR2 agonist LTA-SA (*SI Appendix*, Fig. S5*D*).

Given the increased expression of ACOD1 in mitochondria upon Mtb infection and the reported ability of ACOD1 (49) and lysosomal enzymes (50) to increase mitochondrial generation of (ROS) (49), we questioned whether mitochondrial ROS generation was contributing to Co-D MD (*SI Appendix*, Fig. S5*E*). However, treatment of the cells with the mitochondrial antioxidant MitoQ (51) at levels up to 500 nM afforded no protection against Mtb-induced cell death, while the pan-caspase inhibitor K777 at a concentration of 10 μM was fully protective (*SI Appendix*, Fig. S5*F*). Thus, mitochondrial ROS generation is unlikely to play a part in ACOD1's promotion of Co-D MD.

Discussion

Our findings, summarized in *SI Appendix*, Fig. S6, add lysosome-dependent cell death to the ways in which various investigators have found macrophages to succumb to Mtb, as reviewed in ref. 1. Lysosome-dependent cell death appears to be the predominant cell death mechanism driven by type I IFN produced by Mtb-infected macrophages. By itself, type I IFN does not kill macrophages. Co-D MD requires an additional effect of Mtb infection besides induction of type I IFN. Given the critical role of lysosome membrane permeability in Co-D MD, we speculate that this additional effect may be Mtb's ability to damage phagolysosomal membranes, such as through secretion of the pore-forming proteins ESAT-6 and Cfp10 (35, 52–55). Lysosome membrane permeabilization has been observed in macrophages infected with Mtb (56–59). We speculate that lysosome-dependent cell death may be the fate of macrophages infected with other pathogens that also induce high expression of ACOD1 and damage phagolysosomal membranes. We found striking protection of macrophages from lysosome-dependent cell death by a pan-cathepsin inhibitor, K777. The same compound protected human macrophages from pyroptosis (35). The protection afforded in our hands by CI-XII likely also resulted from inhibition of multiple cysteine proteases.

Our second major finding was particularly surprising: Co-D MD was largely due to increased expression of ACOD1. *Acod1*$^{-/-}$ mice undergo more Mtb-induced histopathology than wild-type mice (60, 61). The contrast between ACOD1's impact on macrophages in vitro and its impact on the whole mouse highlights the diversity of its actions (46). We confirmed a protective role of ACOD1's product, itaconate, on Mtb-infected macrophages

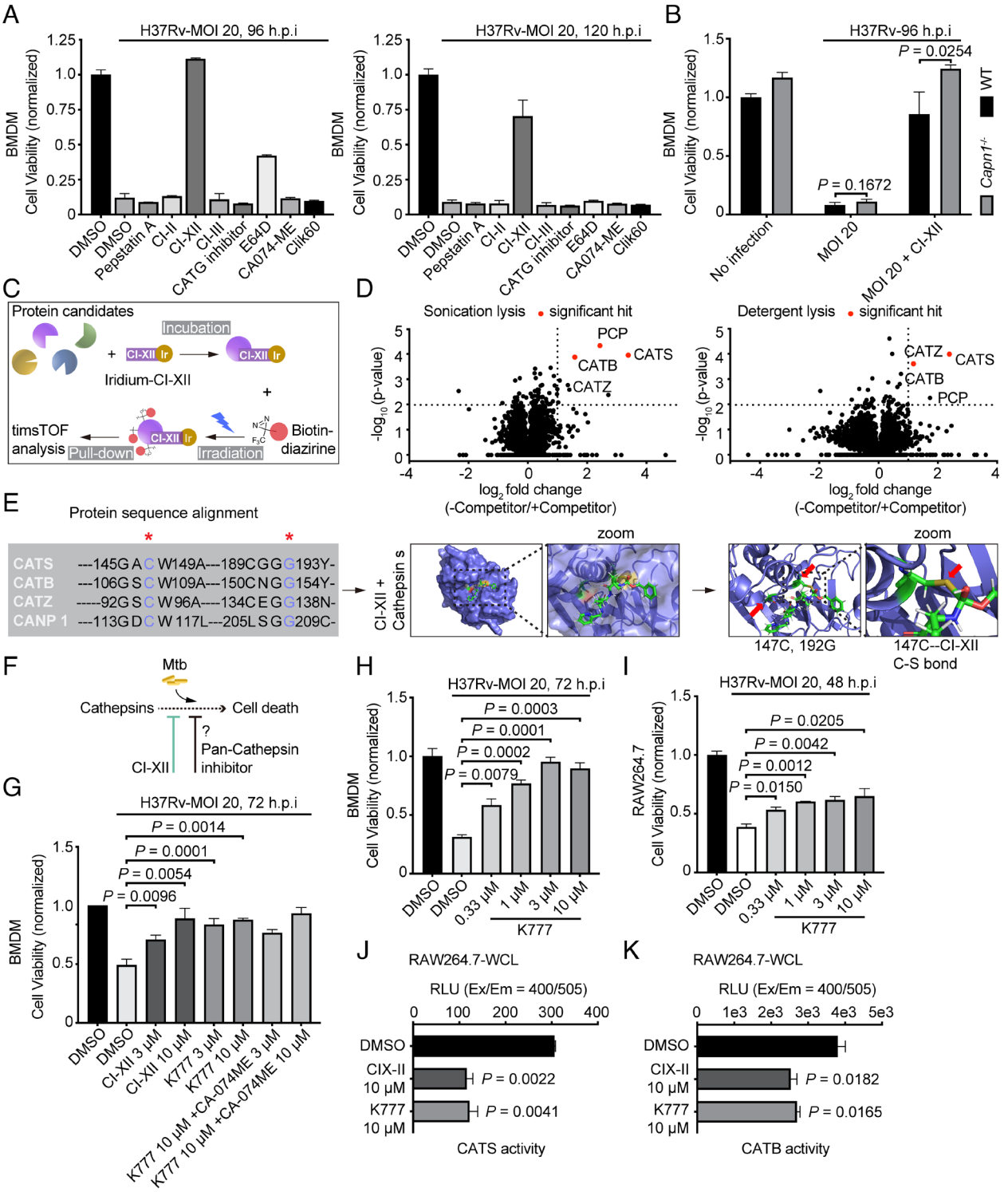

Fig. 3. Pan-cathepsin inhibitors protect macrophages from Mtb-induced death. (*A*) BMDM were pretreated with inhibitors (10 μM) for 2 h before infection of Mtb at an MOI of 20 and treatment was continued throughout the experiment. Cell viability was measured by ATP assay. (*B*) WT and *Capn1*$^{-/-}$ BMDM were treated with DMSO or CI-XII, then infected with Mtb H37Rv as in (*A*) and cell viability assessed 96 h later. (*C*) Schematic representation of the Dexter energy transfer-affinity labeling mass spectrum analysis. Ir, iridium. The structure of the probe is shown in *SI Appendix*, Fig. S3*B*. (*D*) BMDM were lysed via sonication (*Left*) or detergent (*Right*). Ir-CI-XII (1 μM) and biotin-diazirine (250 μM) were added to the lysates and the mixtures were irradiated with 450 nm light for 10 min. Samples were incubated with streptavidin beads and the retentate on washed beads was analyzed by mass spectrometry on a Bruker timsTOF Pro as detailed in (28). (*E*) (*Left*) Multiple protein sequence alignment of mouse cathepsin S (CATS), B (CATB), Z (CATZ), and calpain-1 (CAN1); shown is comparison of partial sequences of indicated proteins. Asterisks (*) indicate conserved residues that form possible contacts with CI-XII. Alignment was processed with MEGA X software. (*Middle*) Docking model of CATS with CI-XII, predicted by Schrödinger software. (*Right*) Demonstration of 147C and 192G residues' locations in the binding pocket of CATS, C–S bond between 147C and CI-XII. (*F*) Schematic representation of hypothesis that K777 may protect Mtb-infected cells. (*G*) BMDM were treated with DMSO, CI-XII, K777, or K777 with CA-074ME at the indicated concentrations, then infected with Mtb H37Rv at MOI 20 before assessing cell viability at the times shown. (*H*) BMDM were treated with DMSO or K777 at the indicated concentrations and infected with Mtb H37Rv at MOI 20 before assessing cell viability 72 h later. (*I*) RAW264.7 cells were treated with DMSO or K777 at the indicated concentrations and infected with Mtb H37Rv at MOI 20 before cell viability was assessed 48 h later. (*J* and *K*) Whole cell lysate (WCL) was prepared from RAW264.7 cells treated with the indicated inhibitors or DMSO as a vehicle control. Equal amounts of protein from each lysate as measured by the BCA protein assay were assessed for CATS or CATB activity by a fluorescent assay. Data in *A*, *B*, *G*–*K* represent mean ± SD of 3 (*G*–*I*) or 2 (*J* and *K*) replicates in 1 experiment representative of 2 independent experiments. *P*-values by the unpaired *t* test.

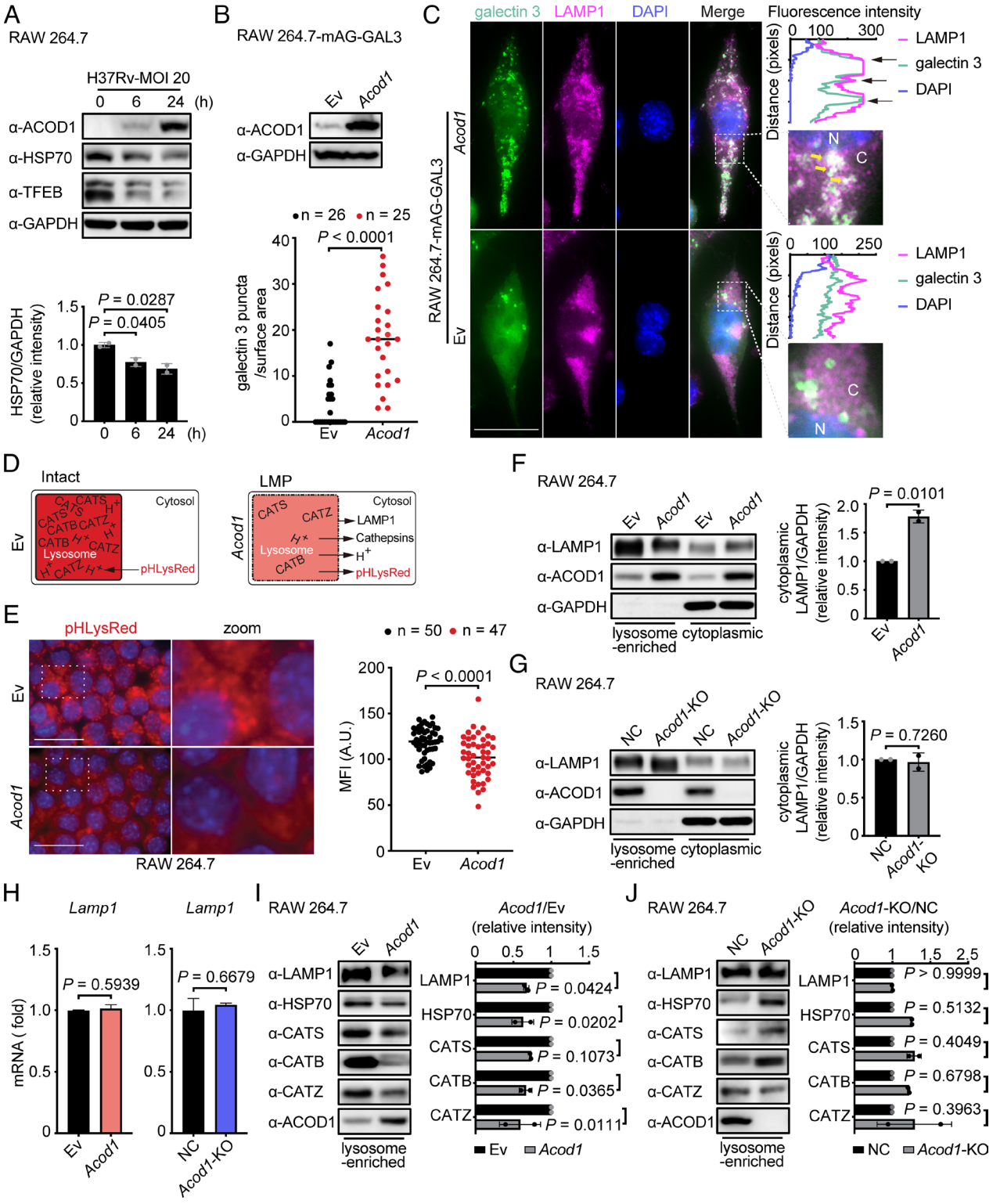

Fig. 4. ACOD1 overexpression mediates lysosomal membrane permeabilization (LMP). (*A*) (*Top*) Immunoblot analysis of RAW264.7 cells infected with Mtb H37Rv at MOI 20 for the indicated times. (*Bottom*) Semiquantification of indicated protein levels, assessed by gray intensity analysis via Image J software. (*B* and *C*) RAW264.7 cells stably expressing GFP-tagged galectin3 (mAG-GAL3) were transiently transfected with Ev- or *Acod1*-encoding plasmids and analyzed by immunoblot and immunofluorescence (IF) microscopy. (Scale bar, 10 μm.) (*B*) (*Top*) Immunoblot analysis of transfected cells. (*Bottom*) Quantification of galectin 3 puncta in the cells shown in (*C*), Ev-expressing cells, n = 26; ACOD1-expressing cells, n = 25. (*C*) IF analysis of transfected cells. (*D*) Schematic models of lysosomes without (intact) and with LMP. (*E*) (*Left*) Ev- or ACOD1-overexpressing RAW264.7 cells were incubated with pHLysRed and analyzed by fluorescence microscopy for pHLysRed distribution. (Scale bar, 20 μm.) (*Right*) Quantification of pHLysRed signal intensity of shown cells via Image J software. MFI, mean fluorescent intensity. Ev-expressing cells, n = 50; ACOD1-expressing cells, n = 47. (*F* and *G*) (*Top Left*, *Bottom Left*) Fractionation immunoblot analysis of Ev- or ACOD1- overexpressing RAW264.7 cells (*F*) and NC or Acod1-KO RAW264.7 cells (*G*). (*Top Right*, *Bottom Right*) Semiquantification of indicated protein levels, assessed by gray intensity analysis via Image J software. (*H*) mRNA level of *Lamp1* in Ev- or ACOD1-overexpressing RAW264.7 cells and NC or *Acod1*-KO RAW264.7 cells, assessed by RT-PCR. (*I*) (*Left*) Fractionation immunoblot analysis of Ev- or ACOD1- overexpressing RAW264.7 cells. (*Right*) Semiquantification of indicated protein levels, assessed by gray intensity analysis via Image J software. (*J*) (*Left*) Fractionation immunoblot analysis of NC or *Acod1*-KO RAW264.7 cells. (*Right*) Semiquantification of indicated protein levels, assessed by gray intensity analysis via Image J software. Data in *A*, *F*–*J* are mean ± SD of 3 replicates in 1 experiment representative of 2 independent experiments. *P*-values by the unpaired *t* test.

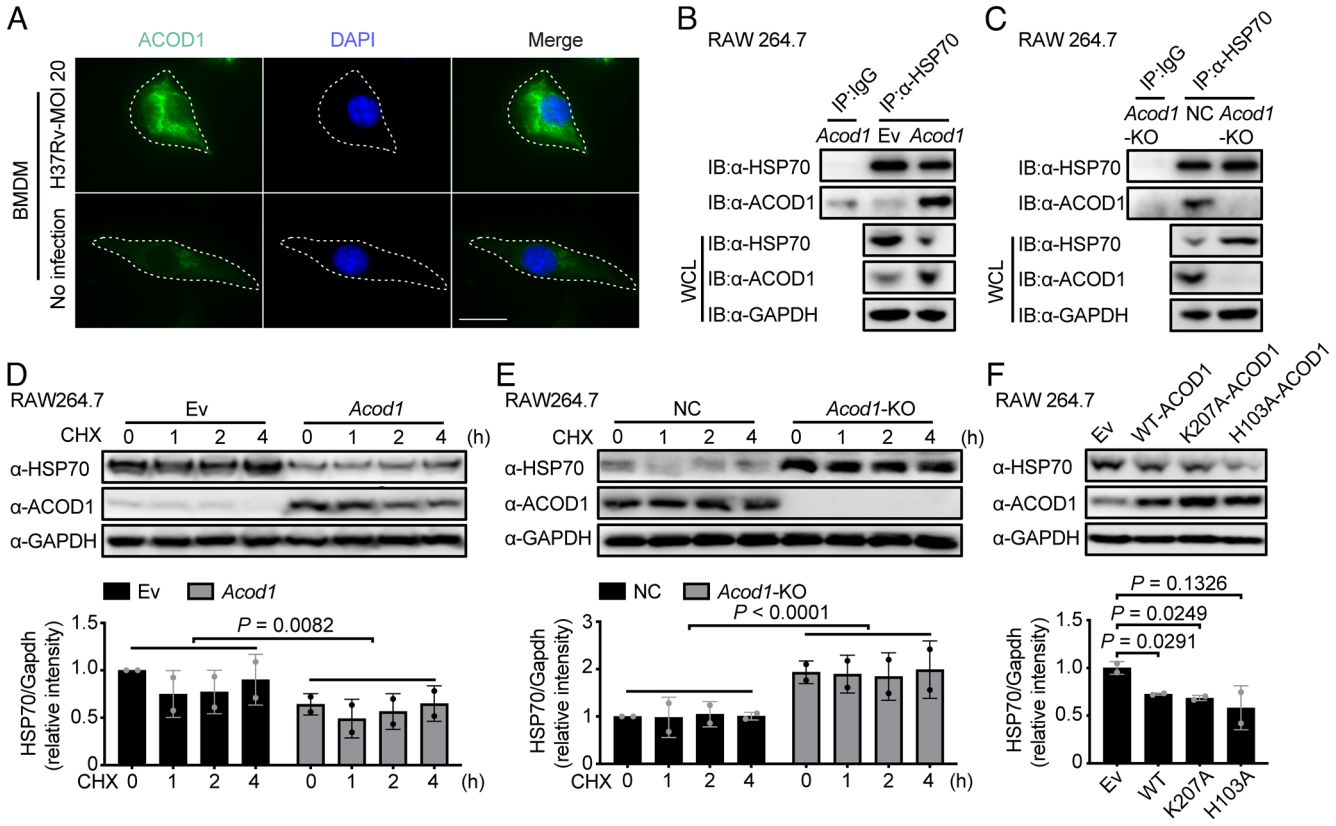

Fig. 5. ACOD1 binds to and decreases the level of HSP70, contributing to LMP. (*A*) BMDM were infected with Mtb H37Rv at MOI 20 for 24 h before cells were visualized by IF microscopy. Dashed lines outline cells. ACOD1 was labeled with anti-ACOD1 antibody and anti-rabbit IgG-488 (Alexa Fluor-tagged) secondary antibody. Nuclei are highlighted with DAPI, a fluorescent stain for DNA. (Scale bar, 10 μm.) (*B*) Coimmunoprecipitation (IP) analysis of Ev- or ACOD1-overexpressing RAW264.7 cells using rabbit anti-HSP70 antibody for pull-down with rabbit IgG as an isotype control, followed by immunoblot (IB) with antibodies against (α) HSP70 or ACOD1, compared to IB of the WCL with those antibodies and antibody against glyceraldehyde 3-phosphate dehydrogenase (GAPDH) as a control. (*C*) As in (*B*) but using lysates of NC or *Acod1*-KO RAW264.7 cells. (*D*) Ev- or ACOD1-overexpressing RAW264.7 cells were treated with 100 μg/ml CHX for indicated times before immunoblot analysis. (*Bottom*) Semiquantification of indicated protein levels, assessed by gray intensity analysis via Image J software. (*E*) As in (*D*) but using lysates from NC or *Acod1*-KO RAW264.7. (*F*) As in (*D*) but using lysates from Ev-, WT-ACOD1-, K207A-ACOD1-, or H103A-ACOD1-overexpressing RAW264.7 cells. Data are means ± SD of 3 replicates representative of 3 (*B* and *C*) or 2 (*D*–*F*) independent experiments. *P*-values by the unpaired *t* test.

in vitro, which could be due to its alkylation of TFEB at Cys212, promoting its nuclear localization (62) and the subsequent transcription of genes involved in lysosomal biogenesis (16), a process that could be augmented in turn by TFEB's reported ability to induce itaconate synthesis (63). However, we found an opposing, noncatalytic role of ACOD1 that had a greater impact on macrophages at the levels of ACOD1 expression that accompanied Mtb infection: promotion of lysosome membrane permeabilization and cell death. An itaconate-independent effect of ACOD1 on TNF signaling has been reported (64), but this did not exclude a role for ACOD1 catalysis other than itaconate production. We are not aware of prior evidence that ACOD1 can act noncatalytically to affect cell fate.

A third major finding was the association of cytosolic ACOD1 with HSP70 and ACOD1's promotion of HSP70's proteasomal degradation. We do not know whether accumulation of ACOD1 in the cytosol results from high-level expression alone or also involves posttranslational modification and/or association with additional proteins besides Hsp70. Given the essential role of HSP70 in stabilizing lysosomes (12, 13, 36–38), the marked decrease in HSP70 levels we observed may add to the phagolysosome-damaging actions of Mtb to bring about lysosome-dependent cell death. A hypothesis we hope to test in future work is that HSP70 may bind to the nascent pores formed by Mtb's pore-forming proteins and prevent them from causing LMP, similar to the role for stress granules described by Bussi et al. (58). The molecular details of ACOD1's association with HSP70, including whether it is direct or mediated by a shared partner(s), remain to be determined, as does the means by which this association leads to HSP70's degradation.

A fourth finding of this study relates to our search for an enzyme(s) induced or activated by type I IFN signaling that might safely be inhibited by a pharmacological agent as an adjunctive HDT for tuberculosis without impairing antiviral defense. For two reasons, ACOD1 is not that enzyme: Its knockout increases the severity of experimental tuberculosis in mice (60, 61) and its deleterious effect on viability of Mtb-infected macrophages is nonenzymatic. Instead, our results direct attention to cysteine proteases acting in a mutually redundant manner. We were unable to test whether CI-XII might protect mice from Mtb, as the compound is highly insoluble, showed only about 3% and 15% bioavailability after administration by oral and intraperitoneal routes, respectively, and was cleared rapidly from the blood (*SI Appendix*, Fig. S7). K777 is also highly insoluble. Future work might identify a more drug-like, broad-spectrum cysteine protease inhibitor. However, pursuing cathepsin inhibitors for treatment of tuberculosis would likely be problematic, given that certain cathepsin inhibitors promoted macrophage death (65), knockdown of *Ctss*, *Ctsb,* or *Ctsl* increased the survival of Mtb in human macrophages (66), and toxicity from on-target and off-target effects could be considerable. Instead, we plan to focus on how we might disrupt ACOD1's interaction with HSP70.

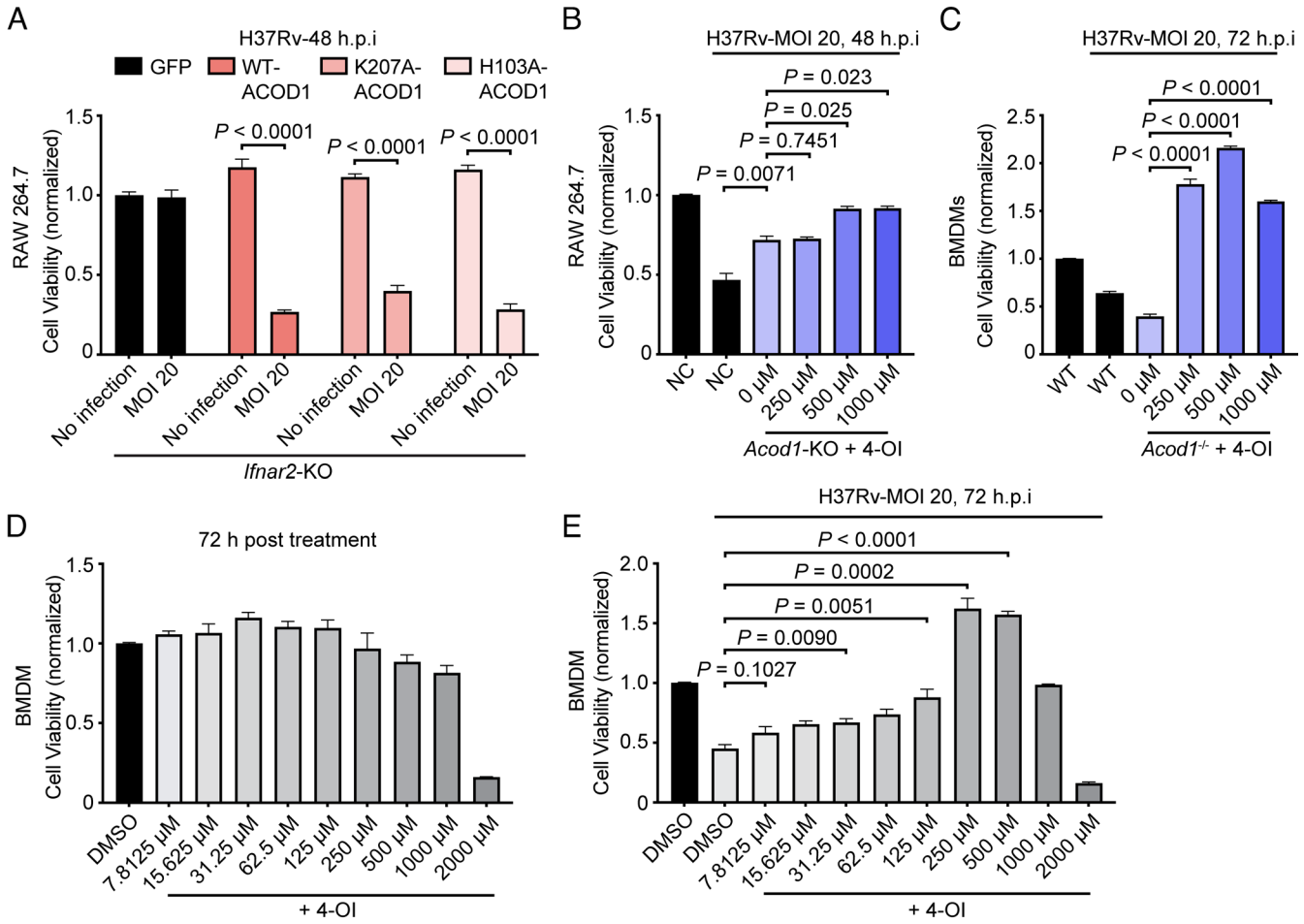

Fig. 6. ACOD1 mediates Mtb-induced cell death independently of catalysis and itaconate. (*A*) GFP-, WT-ACOD1-, K207A-ACOD1-, or H103A-ACOD-overexpressing *Ifnar2*-KO RAW264.7 cells were infected or not with Mtb H37Rv at MOI 20 and their viability assessed 48 h later. (*B*) *Acod1*-KO RAW264.7 cells were treated with the indicated concentrations of 4-OI for 2 h before Mtb infection (and were treated with 4-OI during infection). Then they and NC RAW264.7 cells were infected or not with Mtb H37Rv at MOI 20. Cell viability was assessed 48 h later. (*C*) *Acod1*$^{-/-}$ BMDM were treated with the indicated concentrations of 4-OI for 2 h before Mtb infection (and were treated with 4-OI during infection). Then they and WT BMDM were infected or not with Mtb H37Rv at MOI 20 and their viability was assessed 72 h later. (*D*) BMDM from WT mice were treated with 4-OI in the indicated concentrations for 72 h and cell viability was assessed. (*E*) BMDM from WT mice were treated with 4-OI in the indicated concentrations for 2 h before Mtb infection (and were treated with 4-OI during infection), then infected or not with Mtb H37Rv at MOI 20. Cell viability was assessed 72 h later. Data in *A*–*E* represent mean ± SD of 3 replicates in 1 experiment representative of 2 (*A*–*D*) or 3 (*E*) independent experiments. *P*-values by the unpaired *t* test.

Materials and Methods

Mice and BMDM. WT C57BL/6 ("B6") (#000664), 129X1(# 000691), and Acod1$^{-/-}$ (#029340) female mice on the C57BL/6 background were from Jackson Laboratory. Female 129S2 mice (#476) were from Charles River Laboratories. Femurs from calpain-1 KO mice were a kind gift of Dr. Michel Baudry, Western University of Health Sciences, Pomona, Ca. Mice were housed in specific-pathogen-free (SPF) facility. All animal work was approved by and proceeded in accordance with the requirements of Weill Cornell Medicine Institutional Animal Care and Use Committee. Femurs were sterilized by dipping in ice-cold 75% ethanol, then rinsed with PBS and DMEM. BMDM precursors were flushed from femurs with DMEM and centrifuged at 193 g for 8 min at room temperature. Cells were resuspended in DMEM supplemented with 20% L929-conditioned medium (LCM), 10% fetal bovine serum (FBS), 1 mM sodium pyruvate, 2 mM L-glutamine, and 10 mM HEPES (pH 7.5) (BMDM medium) and cultured in 5% CO_2 in air at 37 °C for 7 d. The adherent BMDM were detached by gentle pipetting in ice-cold PBS with 1 mM EDTA, washed once with ice-cold PBS and resuspended and cultured in BMDM medium.

Cell Culture. HEK293T, RAW264.7-WT cells (from BEI Resources) and RAW264.7-derived overexpression or gene knock-out cells were cultured in DMEM (Gibco™, #11965092) supplemented with 10% fetal bovine serum (FBS), 1 mM sodium pyruvate, 2 mM L-glutamine, and 10 mM HEPES (pH 7.5) in 5% CO_2 in air at 37 °C.

Lysosomal pH Detection. RAW264.7-TetOne-Ev and RAW264.7-TetOne-Acod1 cells were seeded in a 4-well Falcon® CultureSlide for 2 h and then treated with 20 ng/ml doxycycline for 24 to 36 h to induce ACOD1 overexpression. Cells were then carefully washed with HBSS and incubated with pHLysRed dye (DOJINDO, #L265) at 37 °C for 30 min according to the manufacturer's protocol followed by incubation with NucBlue™ Live ReadyProbes™ Reagent for nuclear staining and prepared as above for imaging with a Keyence BZ-X800 system.

Cell Viability Assay. Macrophage viability was assessed by measuring ATP levels with CellTiter-Glo® Luminescent Cell Viability Assay kit (Promega, #G7570) according to the manufacturer's protocol and expressed as a percent of the value for uninfected cells.

Cathepsin activity assay. Cathepsin activity in cell lysates was evaluated with Cathepsin B Activity Assay Kit (Fluorometric) (Abcam, ab65300) and Cathepsin S Activity Assay Kit (Fluorometric) (Abcam, ab65307) according to the manufacturer's protocols.

Statistical Analysis. Statistical analyses were performed with GraphPad Prism 9 software. Data are presented as mean ± SD. *P* values were calculated via the two-tailed unpaired *t* test, two-way ANOVA (Šídák's multiple comparisons test) as specified in the figure legends. *P* values < 0.05 were considered statistically significant.

SI Appendix details *Materials and Methods* for Mtb culture and infection, lentivirus preparation and transfection, generation of knockout cells and cells engineered for doxycycline-induced overexpression, sourcing of antibodies and reagents, preparation of subcellular fractions, coimmunoprecipitation, immunoblotting, molecular docking, PCRs, immunofluorescent imaging, and pharmacokinetic determination.

Data, Materials, and Software Availability. RNAseq results data have been deposited in GEO (GSE289356) (67). All study data are included in the article and/or supporting information.

ACKNOWLEDGMENTS. We thank Drs. Michel Baudry and Yan Liu (Western University of the Health Sciences, Pomona, CA) for calpain-1 KO cells, Daqiang Li and Gang Lin (Weill Cornell Medicine) for advice and help with the docking study, and Jennifer Hanna (Center for Discovery and Innovation, Hackensack Meridian Health) for help with pharmacokinetics. Extensive pull-down work not included here was performed by S.O. This work was funded by NIH Grant R21AI178133 to C.N., R01AI155510 to J.A., a Cancer Research Institute fellowship to L.Z., and the Abby and Howard P. Milstein Program in Chemical Biology and Translational Medicine. The Department of Microbiology and Immunology at Weill Cornell Medicine is supported by the William Randolph Hearst Foundation.

Author affiliations: [a]Department of Microbiology and Immunology, Weill Cornell Medicine, New York, NY 10065; [b]Department of Immunology and Microbiology, School of Life Sciences, Southern University of Science and Technology, Shenzhen, Guangdong 518055, China; [c]Division of Chemical Biology and Medicinal Chemistry, University of North Carolina Eshelman School of Pharmacy, University of North Carolina at Chapel Hill, Chapel Hill, NC 27599; [d]Department of Pharmacology, Weill Cornell Medicine, New York, NY 10065; and [e]Center for Discovery and Innovation, Hackensack Meridian Health, Nutley, NJ 07110

1. L. Zhang, X. Jiang, D. Pfau, Y. Ling, C. F. Nathan, Type I interferon signaling mediates *Mycobacterium tuberculosis*-induced macrophage death. *J. Exp. Med.* **18**, e20200887 (2021).
2. A. M. Lee, C. F. Nathan, Type I interferon exacerbates *Mycobacterium tuberculosis* induced human macrophage death. *EMBO Rep.* **25**, 3064–3089 (2024).
3. Y. J. Crow, J. L. Casanova, Human life within a narrow range: The lethal ups and downs of type I interferons. *Sci. Immunol.* **9**, eadm8185 (2024).
4. P. Bastard *et al.*, A loss-of-function IFNAR1 allele in Polynesia underlies severe viral diseases in homozygotes. *J. Exp. Med.* **219** (2022).
5. F. McNab, K. Mayer-Barber, A. Sher, A. Wack, A. O'Garra, Type I interferons in infectious disease. *Nat. Rev. Immunol.* **15**, 87–103 (2015).
6. J. B. Geri *et al.*, Microenvironment mapping via Dexter energy transfer on immune cells. *Science* **367**, 1091–1097 (2020).
7. P. Boya, Lysosomal function and dysfunction: Mechanism and disease. *Antioxid Redox Signal* **17**, 766–774 (2012).
8. P. Boya, G. Kroemer, Lysosomal membrane permeabilization in cell death. *Oncogene* **27**, 6434–6451 (2008).
9. N. Raben, R. Puertollano, TFEB and TFE3: Linking lysosomes to cellular adaptation to stress. *Annu. Rev. Cell Dev. Biol.* **32**, 255–278 (2016).
10. F. Wang, R. Gomez-Sintes, P. Boya, Lysosomal membrane permeabilization and cell death. *Traffic* **19**, 918–931 (2018).
11. A. Michelucci *et al.*, Immune-responsive gene 1 protein links metabolism to immunity by catalyzing itaconic acid production. *Proc. Natl. Acad. Sci. U.S.A.* **110**, 7820–7825 (2013).
12. H. L. Chiang, S. R. Terlecky, C. P. Plant, J. F. Dice, A role for a 70-kilodalton heat shock protein in lysosomal degradation of intracellular proteins. *Science* **246**, 382–385 (1989).
13. T. Kirkegaard *et al.*, Hsp70 stabilizes lysosomes and reverts Niemann-Pick disease-associated lysosomal pathology. *Nature* **463**, 549–553 (2010).
14. A. F. McGettrick, L. A. Bourner, F. C. Dorsey, L. A. J. O'Neill, Metabolic messengers: Itaconate. *Nat. Metab.* **6**, 1661–1667 (2024).
15. A. Swain *et al.*, Comparative evaluation of itaconate and its derivatives reveals divergent inflammasome and type I interferon regulation in macrophages. *Nat. Metab.* **2**, 594–602 (2020).
16. M. Sardiello *et al.*, A gene network regulating lysosomal biogenesis and function. *Science* **325**, 473–477 (2009).
17. R. Bryk *et al.*, Potentiation of rifampin activity in a mouse model of tuberculosis by activation of host transcription factor EB. *PLoS Pathog* **16**, e1008567 (2020).
18. C. C. B. Bomfim *et al.*, *Mycobacterium tuberculosis* induces Irg1 in murine macrophages by a pathway involving both TLR-2 and STING/IFNAR signaling and requiring bacterial phagocytosis. *Front. Cell Infect. Microbiol.* **12**, 862582 (2022).
19. Z. Li *et al.*, Novel peptidyl alpha-keto amide inhibitors of calpains and other cysteine proteases. *J. Med. Chem.* **39**, 4089–4098 (1996).
20. H. R. Momeni, Role of calpain in apoptosis. *Cell J.* **13**, 65–72 (2011).
21. F. Urthaler, P. E. Wolkowicz, S. B. Digerness, K. D. Harris, A. A. Walker, MDL-28170, a membrane-permeant calpain inhibitor, attenuates stunning and PKC epsilon proteolysis in reperfused ferret hearts. *Cardiovasc Res.* **35**, 60–67 (1997).
22. K. Doh-Ura, T. Iwaki, B. Caughey, Lysosomotropic agents and cysteine protease inhibitors inhibit scrapie-associated prion protein accumulation. *J. Virol.* **74**, 4894–4897 (2000).
23. T. Yamashima *et al.*, Inhibition of ischaemic hippocampal neuronal death in primates with cathepsin B inhibitor CA-074: A novel strategy for neuroprotection based on "calpain-cathepsin hypothesis". *Eur. J. Neurosci.* **10**, 1723–1733 (1998).
24. D. M. Zhu, F. M. Uckun, Calpain inhibitor II induces caspase-dependent apoptosis in human acute lymphoblastic leukemia and non-Hodgkin's lymphoma cells as well as some solid tumor cells. *Clin. Cancer Res.* **6**, 2456–2463 (2000).
25. K. von der Helm, L. Gurtler, J. Eberle, F. Deinhardt, Inhibition of HIV replication in cell culture by the specific aspartic protease inhibitor pepstatin A. *FEBS Lett.* **247**, 349–352 (1989).
26. M. N. Greco *et al.*, Nonpeptide inhibitors of cathepsin G: Optimization of a novel beta-ketophosphonic acid lead by structure-based drug design. *J. Am. Chem. Soc.* **124**, 3810–3811 (2002).
27. K. Saegusa *et al.*, Cathepsin S inhibitor prevents autoantigen presentation and autoimmunity. *J. Clin. Invest.* **110**, 361–369 (2002).
28. S. A. Ottavi, Efforts toward the discovery and development of novel tuberculosis therapeutics. PhD thesis, (University of North Carolina, ProQuest Dissertations and Theses Global, 2023).
29. U. P. Fonovic *et al.*, Structure-activity relationships of triazole-benzodioxine inhibitors of cathepsin X. *Eur. J. Med. Chem.* **193**, 112218 (2020).
30. Z. Wu *et al.*, Discovery of a new class of potent prolylcarboxypeptidase inhibitors derived from alanine. *Bioorg Med. Chem. Lett.* **22**, 1774–1778 (2012).
31. D. Cuerrier, T. Moldoveanu, J. Inoue, P. L. Davies, R. L. Campbell, Calpain inhibition by alpha-ketoamide and cyclic hemiacetal inhibitors revealed by X-ray crystallography. *Biochemistry* **45**, 7446–7452 (2006).
32. L. Troeberg *et al.*, Cysteine proteinase inhibitors kill cultured bloodstream forms of Trypanosoma brucei brucei. *Exp. Parasitol.* **91**, 349–355 (1999).
33. S. C. Barr *et al.*, A cysteine protease inhibitor protects dogs from cardiac damage during infection by *Trypanosoma cruzi*. *Antimicrob. Agents Chemother.* **49**, 5160–5161 (2005).
34. D. M. Mellott *et al.*, A clinical-stage cysteine protease inhibitor blocks SARS-CoV-2 infection of human and monkey cells. *ACS Chem. Biol.* **16**, 642–650 (2021).
35. K. S. Beckwith *et al.*, Plasma membrane damage causes NLRP3 activation and pyroptosis during *Mycobacterium tuberculosis* infection. *Nat. Commun.* **11**, 2270 (2020).
36. J. Nylandsted *et al.*, Heat shock protein 70 promotes cell survival by inhibiting lysosomal membrane permeabilization. *J. Exp. Med.* **200**, 425–435 (2004).
37. C. Bivik, I. Rosdahl, K. Ollinger, Hsp70 protects against UVB induced apoptosis by preventing release of cathepsins and cytochrome c in human melanocytes. *Carcinogenesis* **28**, 537–544 (2007).
38. M. Gyrd-Hansen, J. Nylandsted, M. Jaattela, Heat shock protein 70 promotes cancer cell viability by safeguarding lysosomal integrity. *Cell Cycle* **3**, 1484–1485 (2004).
39. J. Jia *et al.*, Galectin-3 coordinates a cellular system for lysosomal repair and removal. *Dev. Cell* **52**, 69–87.e68 (2020).
40. S. Chauhan *et al.*, TRIMs and galectins globally cooperate and TRIM16 and galectin-3 co-direct autophagy in endomembrane damage homeostasis. *Dev. Cell* **39**, 13–27 (2016).
41. S. Aits *et al.*, Sensitive detection of lysosomal membrane permeabilization by lysosomal galectin puncta assay. *Autophagy* **11**, 1408–1424 (2015).
42. D. J. Kuhn *et al.*, Potent activity of carfilzomib, a novel, irreversible inhibitor of the ubiquitin-proteasome pathway, against preclinical models of multiple myeloma. *Blood* **110**, 3281–3290 (2007).
43. T. R. Porras-Yakushi, J. M. Reitsma, M. J. Sweredoski, R. J. Deshaies, S. Hess, In-depth proteomic analysis of proteasome inhibitors bortezomib, carfilzomib and MG132 reveals that mortality factor 4-like 1 (MORF4L1) protein ubiquitylation is negatively impacted. *J. Proteomics* **241**, 104197 (2021).
44. J. Santo-Domingo, N. Demaurex, Perspectives on: SGP symposium on mitochondrial physiology and medicine: The renaissance of mitochondrial pH. *J. Gen Physiol.* **139**, 415–423 (2012).
45. F. Chen *et al.*, Crystal structure of cis-aconitate decarboxylase reveals the impact of naturally occurring human mutations on itaconate synthesis. *Proc. Natl. Acad. Sci. U.S.A.* **116**, 20644–20654 (2019).
46. C. G. Peace, L. A. O'Neill, The role of itaconate in host defense and inflammation. *J. Clin. Invest.* **132**, e148548 (2022).
47. D. Degrandi, R. Hoffmann, C. Beuter-Gunia, K. Pfeffer, The proinflammatory cytokine-induced IRG1 protein associates with mitochondria. *J. Interferon. Cytokine Res.* **29**, 55–67 (2009).
48. J. Naujoks *et al.*, IFNs modify the proteome of legionella-containing vacuoles and restrict infection via IRG1-derived itaconic acid. *PLoS Pathog* **12**, e1005408 (2016).
49. C. J. Hall *et al.*, Immunoresponsive gene 1 augments bactericidal activity of macrophage-lineage cells by regulating beta-oxidation-dependent mitochondrial ROS production. *Cell Metab* **18**, 265–278 (2013).
50. M. Zhao, F. Antunes, J. W. Eaton, U. T. Brunk, Lysosomal enzymes promote mitochondrial oxidant production, cytochrome c release and apoptosis. *Eur. J. Biochem.* **270**, 3778–3786 (2003).
51. S. Miriyala *et al.*, Manganese superoxide dismutase, MnSOD and its mimics. *Biochim. Biophys. Acta* **1822**, 794–814 (2012).
52. N. van der Wel *et al.*, *M. tuberculosis and M. leprae* translocate from the phagolysosome to the cytosol in myeloid cells. *Cell* **129**, 1287–1298 (2007).
53. R. Simeone *et al.*, Phagosomal rupture by *Mycobacterium tuberculosis* results in toxicity and host cell death. *PLoS Pathog* **8**, e1002507 (2012).
54. R. Simeone *et al.*, Cytosolic access of *Mycobacterium tuberculosis*: Critical impact of phagosomal acidification control and demonstration of occurrence in vivo. *PLoS Pathog* **11**, e1004650 (2015).
55. J. Augenstreich *et al.*, ESX-1 and phthiocerol dimycocerosates of *Mycobacterium tuberculosis* act in concert to cause phagosomal rupture and host cell apoptosis. *Cell Microbiol.* **19**, 28095608 (2017).
56. E. P. Amaral *et al.*, Lysosomal cathepsin release is required for NLRP3-inflammasome activation by *Mycobacterium tuberculosis* in infected macrophages. *Front. Immunol.* **9**, 1427 (2018).
57. C. Bussi *et al.*, Lysosomal damage drives mitochondrial proteome remodelling and reprograms macrophage immunometabolism. *Nat. Commun.* **13**, 7338 (2022).
58. C. Bussi *et al.*, Stress granules plug and stabilize damaged endolysosomal membranes. *Nature* **623**, 1062–1069 (2023).
59. C. Bussi *et al.*, Publisher correction: Stress granules plug and stabilize damaged endolysosomal membranes. *Nature* **624**, E3 (2023).

60. S. Nair *et al.*, Irg1 expression in myeloid cells prevents immunopathology during M. tuberculosis infection. *J. Exp. Med.* **215**, 1035–1045 (2018).
61. B. I. Machelart *et al.*, IRG1 controls host responses to restrict Mycobacterium tuberculosis infection. bioRxiv [Preprint] (2022). https://doi.org/10.1101/761551 (Accessed 26 September 2024).
62. Z. Zhang *et al.*, Itaconate is a lysosomal inducer that promotes antibacterial innate immunity. *Mol. Cell* **82**, 2844–2857.e2810 (2022).
63. E. M. Schuster *et al.*, TFEB induces mitochondrial itaconate synthesis to suppress bacterial growth in macrophages. *Nat. Metab* **4**, 856–866 (2022).
64. R. Wu *et al.*, Aconitate decarboxylase 1 is a mediator of polymicrobial sepsis. *Sci. Transl. Med.* **14**, eabo2028 (2022).
65. S. J. Salpeter *et al.*, A novel cysteine cathepsin inhibitor yields macrophage cell death and mammary tumor regression. *Oncogene* **34**, 6066–6078 (2015).
66. D. Pires *et al.*, Role of Cathepsins in *Mycobacterium tuberculosis* survival in human macrophages. *Sci. Rep.* **6**, 32247 (2016).
67. L. Zhang, C. F. Nathan, Effects of type I IFN signaling on gene expression of Mycobacterium tuberculosis-infected bone marrow-derived macrophages (BMDMs). GEO. https://www.ncbi.nlm.nih.gov/geo/query/acc.cgi?acc=GSE289356. Deposited 12 February 2025.